UDC 551.509.313:551.511.33

ON THE TRANSIENT BEHAVIOR OF ASAI'S MODEL OF MOIST CONVECTION

ROBERT E. SCHLESINGER and JOHN A. YOUNG
University of Wisconsin, Madison, Wis.

ABSTRACT

The transient behavior of the simple model of moist convection devised by Asai is studied. It is shown that the initial behavior of convective disturbances depends strongly upon the geometry of the disturbance, its initial buoyancy, and dissipative mechanisms. Final approach to a steady convective cell is dependent upon the relative importance of entrainment of heat and momentum. These conclusions derived mainly from linear analysis are substantiated by a series of numerical experiments exhibiting the full nonlinear behavior of the system from formative stages to the final steady-state cell.

1. INTRODUCTION

Convection in the earth's atmosphere occurs in many modes of varying complexity. Both dry and moist convective processes involve multiple scales of motion interacting among themselves. Frequently in such systems, it is difficult to identify the basic elements of the process. A possible exception is moist convection, in which the cloud mass may sometimes retain its identity for a relatively long time. In such a situation, it seems reasonable to parameterize the influence of the small-scale fluctuations on the macroelement by some form of mixing length theory. Unfortunately, the resulting system of governing equations resists easy mathematical analysis because of the inherent nonlinearities: the macroscale advection and microscale mixing processes are typically quadratic in form, while the latent heat release is a discontinuous function of the disturbance state.

In view of this complexity, a straightforward approach is to numerically solve an approximate finite-difference version of the complete governing equations. Such an approach was used by Ogura (1963), who studied the development of an axially symmetric moist convective cell toward the steady state.

An expedient alternative to a complex model is to study a simplified model in the hope of gaining insight into one or more basic features of the physical system. For example, Saltzman (1962) used a highly truncated spectral model to study the growth characteristics and steady heat transfer in dry convection. Kuo (1962) found that a nonlinear formulation of the mixing processes played an important role in adjusting unstable disturbances to a steady state of finite-amplitude convection.

A particularly simple model of moist convection with nonlinear mixing was devised by Asai (1967) and subsequently analyzed to determine the influence of cell geometry upon steady heat transport. The present paper is an attempt to complement Asai's study by considering the dynamics of the convection cell as it evolves toward its steady form—a number of questions present themselves. Which initial disturbances approach a final state of cellular convection? For those which do grow, do the fields of motion and temperature develop at the same rate? Do these rates vary as the disturbance amplitude changes?

Section 2 outlines the assumptions and definitions which comprise the convection model. In section 3, the relations between model parameters, initial growth rates, and steady heat flux are investigated. Linear analysis of the equations is used in section 4 to predict the basic transient behavior for initial and final stages. Finally, numerical solutions of the nonlinear equations are presented in section 5 for various initial conditions and entrainment models.

2. THE MODEL

The geometry of Asai's convection model and the chief variables and constants are shown in figure 1 and the following list of pertinent symbols:

r radial coordinate,
z vertical coordinate,
u radial velocity,
w vertical velocity,
a radius of updraft,
b total radius of cell,
c thickness of layer of inward motion,
d total thickness of cell,
g acceleration due to gravity,
Θ mean potential temperature at rest,
θ potential temperature,
θ_e equivalent potential temperature,
σ a/b,
μ c/d,
l_r αa, radial mixing length ($\alpha>0$),
l_z $\alpha d/2$, vertical mixing length,
s_a $-\partial\theta_e/\partial z$ averaged along axis,
s_b $\partial\theta/\partial z$ averaged along axis,
δ s_a/s_b,

$$k_1 \quad (g/\Theta)(1-\sigma^2)/\left[1-\frac{\ln\sigma}{\mu(1-\mu)}(a/d)^2\right],$$

$$k_2 \quad \frac{[2\alpha^2/a(1-\sigma^2)^2]\left[1+(1-\sigma^2)^3\left(\frac{\sigma\ln\sigma}{1-\sigma^2}\right)^2\left(\frac{a}{d}\right)^4/2\mu^3(1-\mu)^3\sigma\right]}{\left[1-\frac{\ln\sigma}{\mu(1-\mu)}\left(\frac{a}{d}\right)^2\right]},$$

$$k_3 \quad s_a-s_b\left(\frac{\sigma^2}{1-\sigma^2}\right),$$

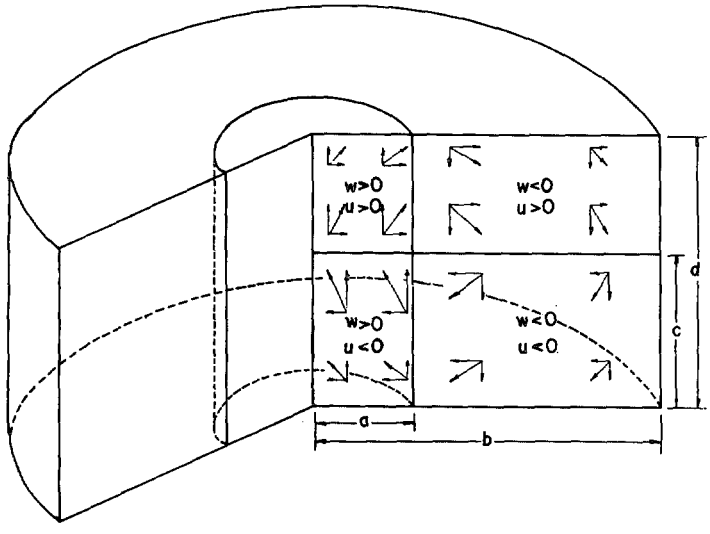

FIGURE 1.—Principal geometrical features of Asai's model of symmetric convection. The vector meridional wind and its components are denoted by arrows in each subregion. The cloudy region is assumed to be $r<a$.

k_4 $[2\alpha^2/a(1-\sigma^2)^2]\left[1+\frac{1-\sigma^2}{\alpha^2}\left(\frac{a}{d}\right)\right]$, and

H $\sigma^2\left(\frac{k_1}{k_2}\right)^{1/2}\left(\frac{k_3}{k_4}\right)^{3/2}$.

Asai's basic assumptions are as follows:

1) The atmosphere is unstable for moist ascending motion ($s_a>0$) and stable for dry descending motion ($s_b>0$).

2) Motion is two-dimensional and cylindrical.

3) All diabatic heating is due to condensation, and evaporation is negligible in the descending current.

4) The total height of the cylinder is much smaller than the atmospheric scale height, so that density variations may be disregarded.

5) $u<0$, $\partial u/\partial z=0$ for $0\leq z<c$; $u>0$, $\partial u/\partial z=0$ for $c<z\leq d$; $w>0$, $\partial w/\partial r=0$ for $0\leq r<a$; $w<0$, $\partial w/\partial r=0$ for $a<r\leq b$.

6) θ increases with height, but at each level assumes separate constant values in the ascending and descending regions.

7) No motion or transport of properties occurs normal to a boundary.

8) A mixing length hypothesis is assumed for eddy transport of heat and momentum as indicated in the list of symbols.

By integrating the thermodynamic equation and the vorticity equation and simplifying the resulting expressions with the help of his assumptions, Asai obtains two ordinary nonlinear differential equations relating the velocity of the updraft to the potential temperature difference between the updraft and the surrounding downdraft:

$$\frac{d\Delta\theta^*}{dt^*}=k_3W^*-k_4\Delta\theta^*W^* \tag{1}$$

and

$$\frac{dW^*}{dt^*}=k_1\Delta\theta^*-k_2W^{*2}. \tag{2}$$

$\Delta\theta^*$ represents the potential temperature difference, averaged both horizontally and vertically, and W^* represents the updraft velocity averaged in the same way; t^* is time. The quantities are starred to emphasize that they are dimensional, in contrast to nondimensionalized quantities which will be defined later. From the list of symbols in section 2, it is apparent that the parameters k_1, k_2, k_3, and k_4 depend strongly upon cell geometry. Apart from this, it should be noted that k_1 and the first term in k_3 are proportional to gravity and the degree of conditional instability, respectively, while k_2 and k_4 are directly proportional to the entrainment coefficient α^2. In equations (1) and (2), k_1 represents thermal buoyancy, and k_3 represents the release of latent heat due to upward motion. The parameters k_2 and k_4, arising from Asai's nonlinear mixing length theory, symbolize the dissipation (via entrainment) of vertical momentum and heat, respectively.

Equations (1) and (2) are identical in form to equations (10) from the article by Kuo (1962) referred to earlier. His convection model is similar to Asai's, except that an absolutely unstable lapse rate is assumed and moisture is not considered. In particular, a nonlinear mixing length theory is adopted. The quantities A and B correspond to W^* and $\Delta\theta^*$; Kuo's parameters k_1, k_2, l_1, and l_2 correspond to Asai's parameters k_1, k_2, k_3, and k_4 in that order.

3. IMPORTANCE OF CELL STRUCTURE AND ENTRAINMENT

Equations (1) and (2) can be linearized by perturbing about a state of rest

$$\Delta\theta^*=\overline{\Delta\theta^*}+\Delta\theta^{*\prime}, \tag{3}$$

$$W^*=\overline{W^*}+W^{*\prime}, \tag{4}$$

$$\overline{\Delta\theta^*}=\overline{W^*}=0, \tag{5}$$

and neglecting products of perturbation terms. The following equations result:

$$\frac{d\Delta\theta^{*\prime}}{dt^*}=k_3W^{*\prime} \tag{6}$$

and

$$\frac{dW^{*\prime}}{dt^*}=k_1\Delta\theta^{*\prime}. \tag{7}$$

When k_3 is positive, as is assumed throughout, equations (6) and (7) have solutions which are linear combinations of e^{Kt^*} and e^{-Kt^*}, where

$$K=\sqrt{k_1k_3}. \tag{8}$$

The e-folding time, the length of time in which the amplifying component e^{Kt^*} grows by a factor of e, is defined by

$$\tau^*=1/\sqrt{k_1k_3}. \tag{9}$$

Figures 2A and 2B exhibit the dependence of τ^* upon the shape of the convective cylinder and upon the conditional instability. As in Asai's article, the thickness of the inflow layer is taken to be half the total thickness to maximize steady-state upward heat transport with respect to μ. A mean potential temperature of 300°K is taken as a reasonable value. The fraction of the area covered by ascending motion is limited by the requirement that k_3 be positive for exponential growth of small perturbations. From Asai's definition of k_3, the cutoff value of σ_c of σ is

$$\sigma_c=\sqrt{\frac{\delta}{1+\delta}}. \tag{10}$$

The solid curves which are nearly horizontal for small σ are isolines of $1/\tau^*$ (1/min). As σ approaches σ_c, the e-folding time tends to infinity since k_3 approaches zero. It is apparent that the greater the instability (the larger δ), the faster the growth of small perturbations from rest while linear theory applies.

The dashed contours in figures 2A and 2B are isolines of a quantity H (°C cm/sec) directly proportional to the steady-state upward heat transport and defined in the list of symbols. Also plotted are the loci of maxima of $1/\tau^*$ and H with respect to σ for a wide range of a/d. Figure 2B indicates that for an updraft with large conditional instability and a horizontal scale comparable to or larger than its vertical scale, the value of σ which maximizes the growth rate of small initial perturbations differs by only a few percent from the value which maximizes the steady-state heat transport, and both these values are nearly independent of a/d. If the instability is small as in figure 2A, the critical values of σ are still virtually independent of a/d, but the correlation between rapid early growth and large steady-state heat transport is much weaker. In narrow updrafts, no such correlation is evident.

The e-folding time is independent of the entrainment strength, but upward heat transport is not. Effects due to varying the entrainment cannot be seen in figure 2, since α^2 is 0.1 in both cases shown. However, if α^2 is increased to 1.0, H becomes an order of magnitude smaller, and the maximizing value of a/d increases by about 40 percent.

Under a wide variety of initial conditions (with certain restrictions to be described later), $\Delta\theta^*$ and W^* tend asymptotically to the nonzero steady-state values obtained formally by setting $d\Delta\theta^*/dt$ and dW^*/dt equal to zero in equations (1) and (2), namely

$$\Delta\theta^*_{SS}=k_3/k_4 \tag{11}$$

and

$$W^*_{SS}=\sqrt{\frac{k_1k_3}{k_2k_4}}. \tag{12}$$

The variation of these values with entrainment intensity, stability, and cell shape for a total thickness of 1 km is demonstrated in tables 1A through 1D. The same assumptions are made as in figures 2A and 2B. Cases (A) and (B) correspond to weak entrainment ($\alpha^2=0.1$), with weak instability ($\delta=0.1$) and strong instability ($\delta=1.0$), respectively. Cases (C) and (D) represent strong entrainment ($\alpha^2=1.0$), again with weak and strong instability in that order. In all cases, the steady-state potential temperature difference $\Delta\theta^*_{SS}$ increases with decreasing σ

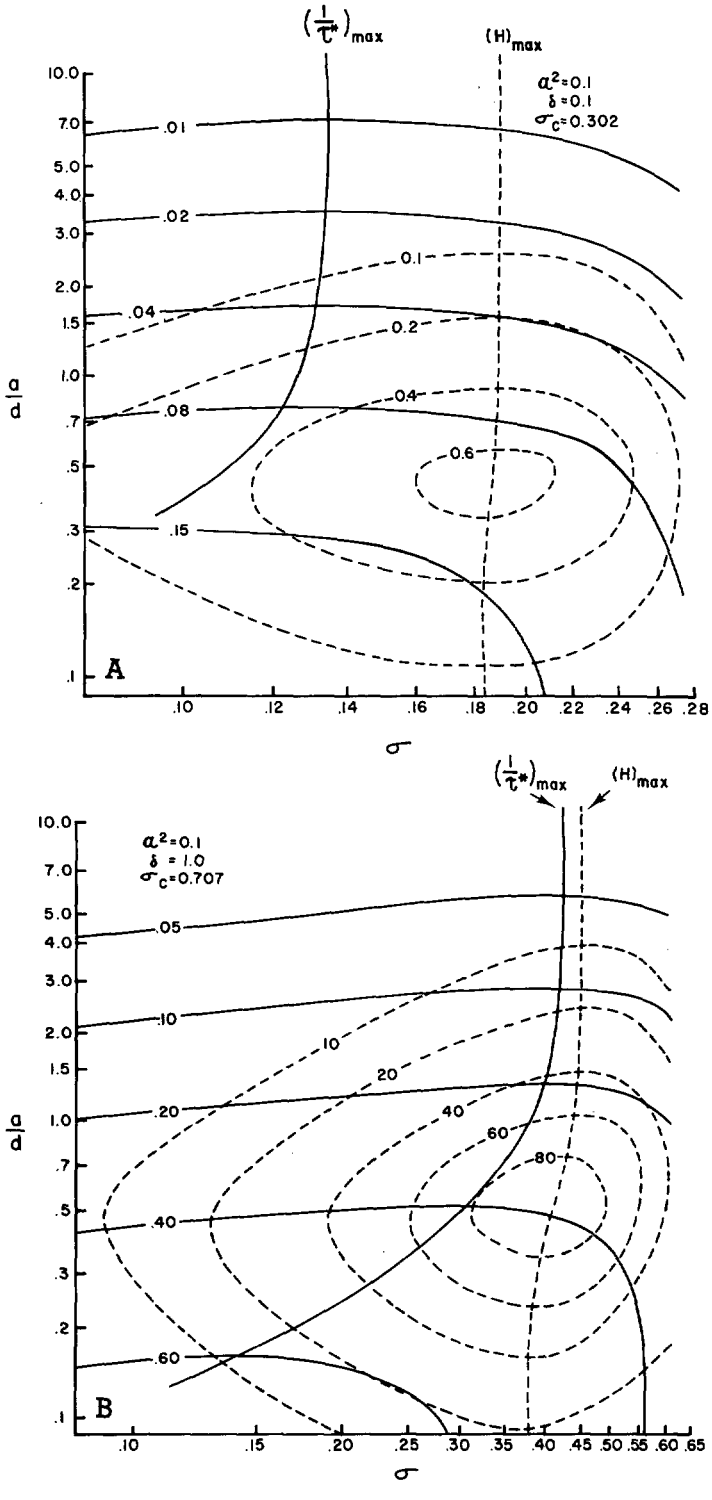

FIGURE 2.—Isolines of H (dashed contours) and $1/\tau^*$ (solid contours) as functions of σ and a/d, as explained in the text; s_b= 3.8°C/km; (A)δ=0.1; (B) δ=1.0.

TABLE 1.—*Steady-state potential temperature difference $\Delta\theta^*_{SS}$ (°K) and upward motion W^*_{SS} (cm/sec) as a function of σ and a/d for $d=1$ km, $\mu=0.5$, $s_b=3.8$°C/km. In each row: upper figures $\Delta\theta^*_{SS}$, lower figures W^*_{SS}*

	$\alpha^2=0.1$, $\delta=0.1$			
a/d \ σ	0.082	0.122	0.183	0.273
11.59	0.17	0.16	0.12	0.03
	11.6	8.7	6.2	2.8
2.86	0.17	0.15	0.12	0.03
	93.0	70.0	49.5	22.3
(A) 1.00	0.16	0.15	0.11	0.03
	331.3	270.4	201.1	92.6
0.350	0.14	0.12	0.09	0.03
	274.4	255.7	214.4	106.5
0.086	0.08	0.07	0.05	0.02
	106.1	99.3	83.5	41.4

	$\alpha^2=0.1$, $\delta=1.0$			
a/d \ σ	0.082	0.159	0.309	0.599
11.59	1.86	1.79	1.53	0.53
	37.9	25.6	17.7	8.7
2.86	1.82	1.75	1.48	0.51
	303.5	205.4	141.8	69.5
(B) 1.00	1.71	1.64	1.39	0.46
	1081.6	822.5	590.9	261.3
0.350	1.46	1.40	1.17	0.37
	895.6	843.9	685.1	233.3
0.086	0.87	0.83	0.68	0.19
	346.3	328.5	265.6	84.3

	$\alpha^2=1.0$, $\delta=0.1$			
a/d \ σ	0.082	0.122	0.183	0.273
11.59	0.16	0.15	0.11	0.03
	3.5	2.7	1.9	0.8
2.86	0.13	0.12	0.09	0.03
	25.7	19.3	13.7	6.1
(C) 1.00	0.09	0.08	0.06	0.02
	77.6	63.2	46.8	21.4
0.350	0.05	0.04	0.03	0.01
	50.0	46.5	38.8	19.1
0.086	0.01	0.01	0.01	0.00
	13.9	13.0	10.9	5.3

	$\alpha^2=1.0$, $\delta=1.0$			
a/d \ σ	0.082	0.159	0.309	0.599
11.59	1.73	1.66	1.41	0.47
	11.5	7.8	5.4	2.6
2.86	1.39	1.33	1.11	0.35
	84.0	56.7	38.8	18.1
(D) 1.00	0.94	0.89	0.73	0.21
	253.3	191.9	135.7	55.5
0.350	0.48	0.46	0.37	0.10
	163.2	153.1	121.9	38.0
0.086	0.15	0.14	0.11	0.03
	45.3	42.8	34.1	10.2

and increasing a/d, so that very broad cells have the strongest thermal development.

The variation of steady-state updraft velocity W^*_{SS} is markedly different in character, as those cells for which σ is small but a is of the order of d have the strongest updrafts. As would be expected qualitatively from continuity arguments, the upward motion decreases with increasing σ since the affected area takes up more of the cell. The updraft velocity falls off relatively rapidly as a is made larger than d, but relatively slowly as a is made smaller than d.

These patterns indicate that in updrafts of comparable horizontal and vertical scale, thermal and kinematic effects are of comparable importance. Predominantly vertical circulations release little heat of condensation in spite of moderate updraft velocities, while predominantly horizontal circulations release the most heat despite small upward velocities.

Tables 1A and 1B, and likewise tables 1C and 1D, are not fully comparable since σ_c is 0.707 for $\delta=1.0$ but only 0.302 for $\delta=0.1$, resulting in considerably different ranges of admissible values for σ. If σ is substantially below 0.3, the tenfold increase in the stability ratio results in an increase of $\Delta\theta^*_{SS}$ by one order of magnitude or slightly more over the tabulated range of a/d, while W^*_{SS} increases by close to half an order of magnitude. Therefore, in Asai's model, the released latent heat in the updraft increases somewhat more strongly with the instability than does the upward motion.

Tables 1A and 1C, and similarly tables 1B and 1D, are completely comparable since each separate pair of tables assumes the same value of δ and hence the same value of σ_c. Both comparisons show that the thermal development decreases drastically with increasing entrainment in narrow updrafts, but by only a few percent in wide updrafts. When α^2 is increased from 0.1 to 1.0, W^*_{SS} drops by nearly a full order of magnitude in narrow updrafts and by about half an order of magnitude in wide ones. Increasing the entrainment intensity in narrow updrafts reduces both the thermal and kinetic development drastically, while in wide updrafts the kinematic development is damped by a factor of 3 with only a slight decrease in the thermal development.

4. THEORETICAL PREDICTIONS

The preceding tables have provided an idea of the variations of growth rates of small initial perturbations about a rest state, and of the actual steady-state temperature difference and updraft velocity in Asai's convection cell for various geometric proportions, entrainment intensities, and stability ratios. It is also instructive to study the effect of initial conditions upon the manner of approach to the steady state (in admissible cases). If dimensionless potential temperature difference, updraft velocity, and time are defined by

$$\Delta\theta=\Delta\theta^*/\Delta\theta^*_{SS}, \tag{13}$$

$$W=W^*/W^*_{SS}, \tag{14}$$

and

$$t=t^*/\tau^*, \tag{15}$$

then the steady-state values of both $\Delta\theta$ and W are unity. The nondimensionalized forms of equations (1) and (2) are

$$\frac{d\Delta\theta}{dt}=\frac{1}{R}(W-W\Delta\theta) \tag{16}$$

and

$$\frac{dW}{dt}=R(\Delta\theta-W^2) \tag{17}$$

where R is a number which depends only upon the dissipative parameters k_2 and k_4:

$$R=\sqrt{k_2/k_4}. \tag{18}$$

Equations (16) and (17) indicate that the growth rates of updraft velocity and potential temperature difference behave inversely with respect to the parameter R. For large values of R, thermal development lags behind kinematic development. In view of the physical meanings of k_2 and k_4, one would expect this inverse relation. Large values of R imply that entrainment dissipates momentum more effectively than it dissipates heat, so that the upward motion approaches the steady state faster than the potential temperature difference does. If R is small, the situation is reversed.

The quantity R does not depend explicitly on the stability ratio, since k_3 is the only one of the four parameters in equations (1) and (2) involving δ. However, k_2 and k_4 depend on a/d and σ, and the larger the value of δ, the greater the cutoff value σ_c. It is, therefore, instructive to investigate the behavior of R with regard to cell geometry, entrainment, and stability.

Table 2 displays the variation of R as a function of σ and a/d for weak, moderate, and strong entrainment as indicated. Again μ is assumed to be 0.5 while δ is unspecified in order to make the three subtables fully comparable. Since R depends on entrainment intensity as well as on cell geometry, any rigid or complete classification of convection modes in terms of R is difficult. Certain tendencies may be inferred, nevertheless, from the definition of R and a comparison of table 2 with table 1 and figure 2:

1) Values of R *much below one* are favored by weak entrainment, radius-to-height ratios of order unity, high updraft speed, and large areas of descending motion. Dissipation of momentum is much less important than dissipation of heat ($k_2<<k_4$).

2) Values of R *substantially greater than one* are favored by strong entrainment, large radius-to-height ratios (wide updrafts), and large values of σ (and, in turn, large conditional instability). Small initial perturbations grow slowly and updraft velocities are low, as might be expected since dissipation of momentum is considerably more important that dissipation of heat ($k_2>k_4$).

3) Apart from transitional modes between those described in 1) and 2), values of R *slightly below one* occur in plumelike updrafts (those which are much narrower than they are tall). The magnitudes of α^2, σ, and δ are of little importance. Small initial perturbations grow rapidly, although the steady-state rising motion is only weak to moderate. Dissipation of momentum and of heat are of nearly equal importance ($k_2=k_4$).

4) R increases with α^2 for each tabulated combination of σ and a/d. Therefore, momentum dissipation becomes more important relative to that of heat as the strength of entrainment is increased.

A more detailed knowledge of the dependence of the growth rates on R can be obtained from linear analysis. Let us now examine the behavior of the nondimensional

TABLE 2.—*Dimensionless parameter R in Asai model as a function of σ and a/d, with μ=0.5*

	$\alpha^2=0.1$			
a/d \ σ	0.086	0.157	0.333	0.607
11.59	0.41	0.65	1.06	1.29
2.86	0.20	0.32	0.51	0.62
1.00	0.14	0.20	0.30	0.36
0.350	0.32	0.35	0.41	0.51
0.086	0.71	0.72	0.74	0.80
0.021	0.91	0.91	0.92	0.94
	$\alpha^2=0.4$			
a/d \ σ	0.086	0.157	0.333	0.607
11.59	0.81	1.28	2.08	2.54
2.86	0.38	0.60	0.97	1.14
1.00	0.25	0.36	0.53	0.61
0.350	0.50	0.54	0.62	0.73
0.086	0.88	0.88	0.90	0.93
0.021	0.97	0.97	0.98	0.98
	$\alpha^2=1.0$			
a/d \ σ	0.086	0.157	0.333	0.607
11.59	1.25	1.97	3.21	3.87
2.86	0.55	0.87	1.40	1.60
1.00	0.34	0.47	0.69	0.76
0.350	0.59	0.64	0.72	0.82
0.086	0.93	0.94	0.95	0.97
0.021	0.99	0.99	0.99	0.99

variables $\Delta\theta$ and W in the vicinity of the steady states of rest ($\Delta\theta=W=0$) and cellular convection ($\Delta\theta=W=1$). After considering first perturbations $\Delta\theta'$ and W' about the state of rest, the linearized equations

$$\frac{d}{dt}(\Delta\theta')=\frac{1}{R}W' \tag{19}$$

and

$$\frac{dW'}{dt}=R\Delta\theta' \tag{20}$$

together with initial perturbation states $\Delta\theta_0'$ and W_0' give the solutions

$$\begin{pmatrix}\Delta\theta'\\ W'\end{pmatrix}=\left(\frac{\Delta\theta_0'R+W_0'}{2R}\right)\begin{pmatrix}1\\ R\end{pmatrix}e^{t} +\left(\frac{\Delta\theta_0'R-W_0'}{2R}\right)\begin{pmatrix}1\\ -R\end{pmatrix}e^{-t}. \tag{21}$$

Interestingly, certain initial states exclude the unstable growth generally implied by the first term on the right-hand side of equation (21). For example, when the buoyancy has the negative value $\Delta\theta_0'=(-1/R)W_0'$, the solutions are simply decaying perturbations toward state of rest:

$$\begin{pmatrix}\Delta\theta'\\ W'\end{pmatrix}=\Delta\theta_0'\begin{pmatrix}1\\ -R\end{pmatrix}e^{-t}. \tag{22}$$

(When $R=1$, it can be readily verified that a similar decay is followed even in the case of finite perturbations in the nonlinear stages.)

If the initial buoyancy is even more negative ($\Delta\theta'_0 < -W'_0/R$), the in-cloud upward motion decreases to zero in a time equal to

$$t=\ln\left[\frac{\Delta\theta'_0 R-W'_0}{\Delta\theta'_0 R+W'_0}\right]^{1/2}.$$

Subsequent times correspond to downward motion in the cloud ($W'<0$), in which case the assumption of pseudo-adiabatic motions in the cloudy region is not physically realistic. It then appears that steady convection can never develop from a sufficiently unfavorable thermal field $\Delta\theta'_0 < -(1/R)W'_0$.

When the initial state exhibits positive buoyancy, the final state would always appear to be one of steady, finite amplitude convection. This is especially suggested in the case $\Delta\theta'_0=W'_0/R$ when only the amplifying perturbation is present:

$$\begin{pmatrix}\Delta\theta'\\ W'\end{pmatrix}=\Delta\theta'_0\begin{pmatrix}1\\ R\end{pmatrix}e^t. \tag{23}$$

As all such unstable disturbances grow toward the final state, the nonlinear dissipative terms play a relatively more important role, and the above linear equations do not hold. To understand the approach to steady convection from any nearby state of motion, let us now consider the perturbations $\Delta\hat{\theta}$ and $\hat{W}$ about the steady state $\Delta\theta=W=1$. They are governed by the linearized equations

$$\frac{d}{dt}(\Delta\hat{\theta})=-\frac{1}{R}\Delta\hat{\theta} \tag{24}$$

and

$$\frac{d}{dt}(\hat{W})=R(\Delta\hat{\theta}-2\hat{W}) \tag{25}$$

whose solutions for $R\neq\sqrt{2}/2$ are:

$$\begin{pmatrix}\Delta\hat{\theta}\\ \hat{W}\end{pmatrix}=\frac{R^2\Delta\hat{\theta}_0}{2R^2-1}\begin{pmatrix}2-\frac{1}{R^2}\\ 1\end{pmatrix}e^{-\frac{1}{R}t}+\left(\hat{W}_0-\frac{R^2\Delta\hat{\theta}_0}{2R^2-1}\right)\begin{pmatrix}0\\ 1\end{pmatrix}e^{-2Rt}. \tag{26}$$

$\Delta\hat{\theta}_0$ and $\hat{W}_0$ represent the initial perturbations. When $R=\sqrt{2}/2$ the solutions become

$$\begin{pmatrix}\Delta\hat{\theta}\\ \hat{W}\end{pmatrix}=\begin{bmatrix}\Delta\hat{\theta}_0\\ \hat{W}_0+\frac{\Delta\hat{\theta}_0}{\sqrt{2}}t\end{bmatrix}e^{-\sqrt{2}t}. \tag{27}$$

Since all perturbation modes are seen to decay, the steady convection cell is approached from nearly all states and for all values of R. When $R<<\sqrt{2}/2$, $\hat{W}$ dies later than $\Delta\hat{\theta}$ (that is, the thermal field is the first to approach its steady value). When $R>>\sqrt{2}/2$, the fields of motion and temperature slowly approach the steady state together:

$$\begin{pmatrix}\Delta\hat{\theta}\\ \hat{W}\end{pmatrix}=\Delta\hat{\theta}_0\begin{pmatrix}1\\ 1/2\end{pmatrix}e^{-(1/R)t}. \tag{28}$$

When taken together, these two sets of linear results suggest interesting differences in the evolution of convection cells for different values of R. For example, when $R<<1$, small perturbations rapidly develop their steady thermal state, followed by a slower approach of the field of motion to its final form. When $R>>1$, the W field develops quickly, after which W and $\Delta\theta$ evolve together to the mature state.

Finally, when $R=1$ and with initial positive buoyancy $\Delta\theta'_0=W'$, we have the linear results:

$$\Delta\theta'=\Delta\theta'_0e^t \quad \text{and} \quad W'=W'_0e^t \tag{29}$$

which conceivably lead to

$$\Delta\hat{\theta}=\Delta\hat{\theta}_0e^{-t} \quad \text{and} \quad \hat{W}=\hat{W}_0e^{-t} \tag{30}$$

when $\Delta\hat{\theta}_0=\hat{W}_0<0$, suggesting that W and $\Delta\theta$ grow together at the same rate. This may be verified for the full nonlinear equations in the special case where $W=\Delta\theta$ for all time. The governing equations then reduce to

$$\frac{dW}{dt}=W-W^2 \tag{31}$$

which gives the solution

$$W(t)=\frac{W_0e^t}{(1-W_0)+W_0e^t}=\Delta\theta(t). \tag{32}$$

This solution exhibits initial exponential growth of W and $\Delta\theta$ together, followed by their transition to the final asymptotic approach to steady convection.

5. NUMERICAL SOLUTIONS

In the preceding section, linear theory was used to predict the qualitative features of the initial and final stages of convection. Nonlinear results were obtained for a single, special case only. To extend the results in the nonlinear cases, we consider now the approximate solution of equations (16) and (17) using the four-step Runge-Kutta scheme with time steps $\Delta t=0.1$. The results are obtained for a variety of initial states in the $\Delta\theta$-W plane.

In the first four of the eight cases considered, the combinations of $\Delta\theta_0$ and W_0 represent small perturbations from rest, lying on a circle of radius 0.1 in the $\Delta\theta$-W plane. In the other combinations, large perturbations are represented by placing the initial point on a circle of radius two, so that at least one of $\Delta\theta_0$ and W_0 is appreciably greater than the steady-state value of unity. The inner cylinder

of the cell is assumed to be initially colder than its surroundings in two cases so that the possibility of steady-state convection under such a condition may be explored. (In all cases, W_0 is nonnegative since descending motion in the inner cylinder is not of physical interest.) The sets of initial conditions are as follows:

Case	$\Delta\theta_0$	W_0
1	0. 1000	0. 0000
2	0. 0707	0. 0707
3	0. 0000	0. 1000
4	−0. 0707	0. 0707
5	2. 0000	0. 0000
6	1. 4142	1. 4142
7	0. 0000	2. 0000
8	−1. 4142	1. 4142

The results appear in figures 3–8 as plots of the solution in the phase plane. Figure 3 allows comparison of the solution curves for various values of R. We see that the agreement of the curves with the results predicted in section 4 is good.

Figures 4–8 show how the convection is affected by changes in R when the initial state is held fixed. The different rates of evolution are apparent from the isolines of time indicated in each figure. Cases 6–8 are not included in the figures, but the salient features of all cases will be noted below.

In the first three cases, steady-state convection develops for the range of R considered (from 0.15 to 2.40). The thermal development is generally ahead of the kinematic development when $R<1$, and lags behind the kinematic development when $R>1$. As has been noted, values of R much below unity are associated mostly with very strong steady-state upward motion; the graphs show that such updrafts develop little of their speed until "thermal equilibrium" is nearly achieved. On the other hand, those updrafts which attain only a low velocity have gained about two-thirds of their speed by the time the potential temperature gradient is half established. After some adjustment, the plumelike updrafts (R close to 1) approach the steady-state temperature excess and upward velocity practically in phase. In case 2, where $\Delta\theta_0=W_0$, $\Delta\theta$ and W remain equal for all time for $R=1$ as shown by equation (32).

The early development of convection is markedly different in cases 1 and 3. In the first case, with a small temperature contrast but no vertical motion initially, the rate of change of temperature difference with t is nearly independent of R, while the updraft develops in proportion to R. In case 3, with initial upward motion but no temperature contrast, the early acceleration of the updraft depends very little on R, but the temperature gradient is nearly proportional to R. This suggests that wide updrafts with small steady-state velocities (large R) develop more rapidly from small thermal perturbations than from a slight upward push; narrow updrafts with high velocities (small R) grow faster from a slight upward velocity than from thermal buoyancy. All the curves in case 3 are virtually horizontal for values of t under about 0.5, indicating that the lack of an initial temperature excess temporarily inhibits vertical accelerations, as would be expected from buoyancy arguments.

In case 4, in contrast to the preceding three cases, the initial temperature contrast is negative and steady-state convection develops only if $R<1$. Updraft growth is increasingly inhibited for t smaller than about 2 as R is increased. It is clear that the initial temperature distribution tends to discourage upward motion in the inner cylinder due to negative buoyancy. The steady state is eventually approached provided $R<1$, but the updraft does not accelerate until the temperature gradient reverses, and shows an increasingly pronounced early deceleration as R approaches 1.

The curve for $R=1$ is not shown since the scaling of the graph provides too little room to include isolines of t. For this value of R, the solutions to equations (17) and (18) become singular, and the rest state ($\Delta\theta=W=0$) is approached instead of the steady state ($\Delta\theta=W=1$). At this point, the initial upward push cannot overcome the negative buoyancy, and the convection decays. It can be inferred that the plumelike updrafts, with R only slightly smaller than 1, are almost completely damped before reversing and approaching the steady state. Values of R larger than 1 correspond to physically meaningless solutions of the equations, since both $\Delta\theta$ and W approach $-\infty$ for sufficiently large t. Since R increases with the entrainment coefficient α^2, especially when a/d is large, the initial negative buoyancy in case 4 supports the development of steady-state convection only if the entrainment rate and updraft width are suitably limited. R also increases with σ, so that the domain of descending motion must be large enough in comparison to the updraft for most of the kinetic energy to be confined to the upward motion according to the continuity requirement.

In cases 5 through 7, as in cases 1 through 3, the nonnegative initial temperature difference supports the development of steady-state convection for the range of R considered (from 0.15 to 2.40). The temperature excess in case 5 is initially twice the steady-state value, but there is no vertical motion. For the three smallest values of R (0.15, 0.25, and 0.40), the steady state is approached monotonically. As R is further increased, however, the updraft exceeds its steady-state velocity for sufficiently large t. The overshoot becomes more pronounced as R increases. It may be inferred from tables 1 and 2 that if the updraft is much narrower or much broader than its depth, R will be large enough for this phenomenon to occur. The strong initial heating evidently creates sufficient buoyancy to accelerate the updraft from its initial rest state beyond its steady-state velocity. As R is increased, the points in the $\Delta\theta$-W plane corresponding to the maximum of W move toward the right and generate an envelope. Since the time origin is immaterial, initial values of $\Delta\theta$ and W situated above this envelope would not be expected to lead to the unstable acceleration just described.

In particular, the point $\Delta\theta=W=1.4142$, the initial point in case 6, lies above the envelope. The convection weakens monotonically with time toward the steady

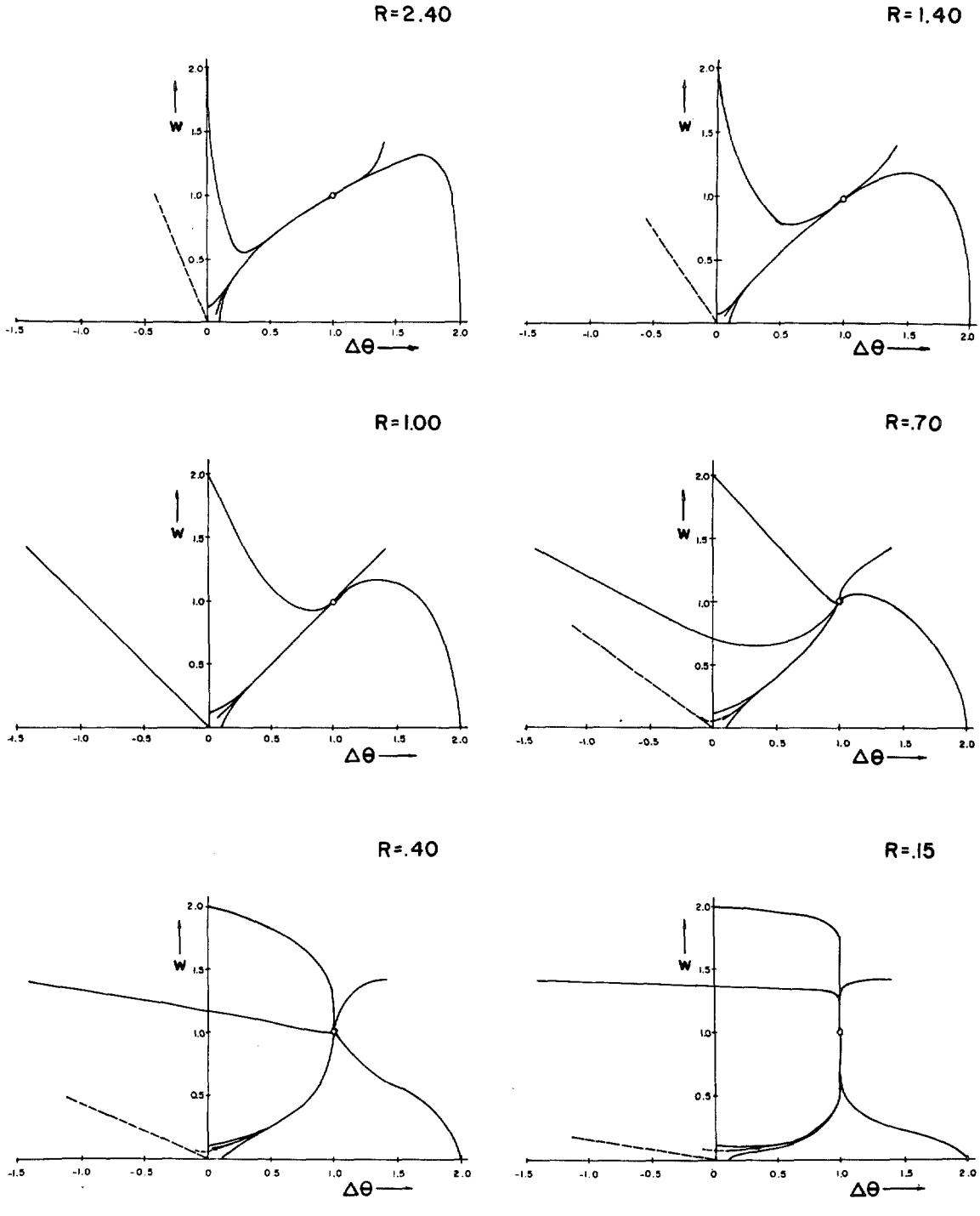

FIGURE 3.—Sets of normalized convection solutions in the phase plane for various values of the parameter R. The state of steady cellular convection is denoted by a circle. The curves show the approach toward the steady state from various initial conditions represented by the free ends.

state for all values of R in case 6. As in case 2, the potential temperature excess approaches the steady state earlier than the updraft velocity if $R<1$, and vice versa if $R>1$.

In case 7, there is no initial temperature gradient, but an updraft having twice the steady-state velocity is assumed. Below a critical value of R slightly less than 0.70, the released heat of condensation creates enough upward buoyancy to prevent the current from decelerating below the steady-state velocity at any time. As R is augmented beyond the critical value, W increasingly undershoots the steady-state value. In view of the rough inverse relationship between R and the actual steady-state velocity W^*_{ss}, large values of R correspond to weak currents which would not be expected to release heat rapidly. When the decelerating current passes its steady-state speed, the weakness of the upward buoyancy

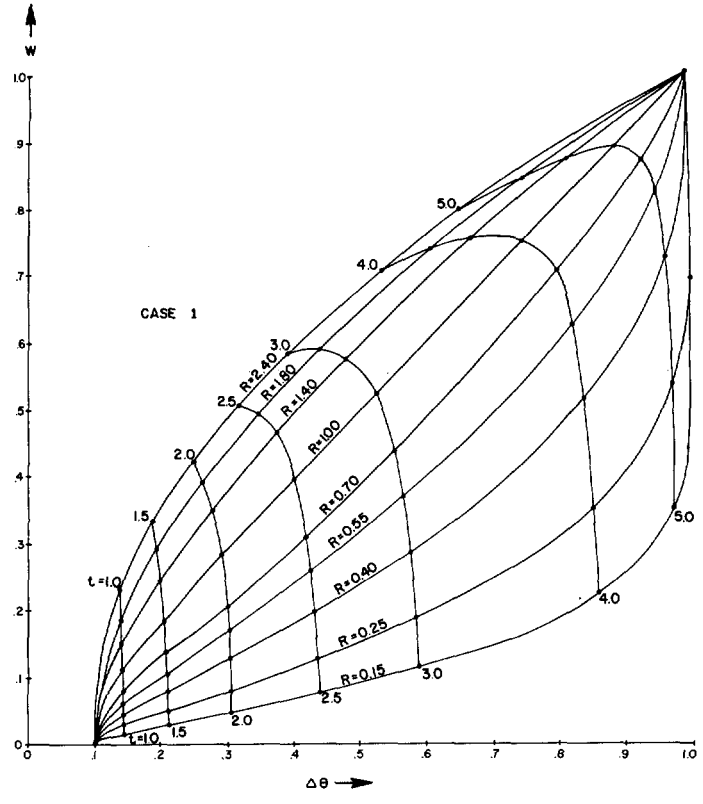

FIGURE 4.—Sets of normalized convection solutions in the phase plane for the initial flow state corresponding to case 1. The various solutions for different values of R are indicated, as are lines connecting equal intervals of time following the initial state.

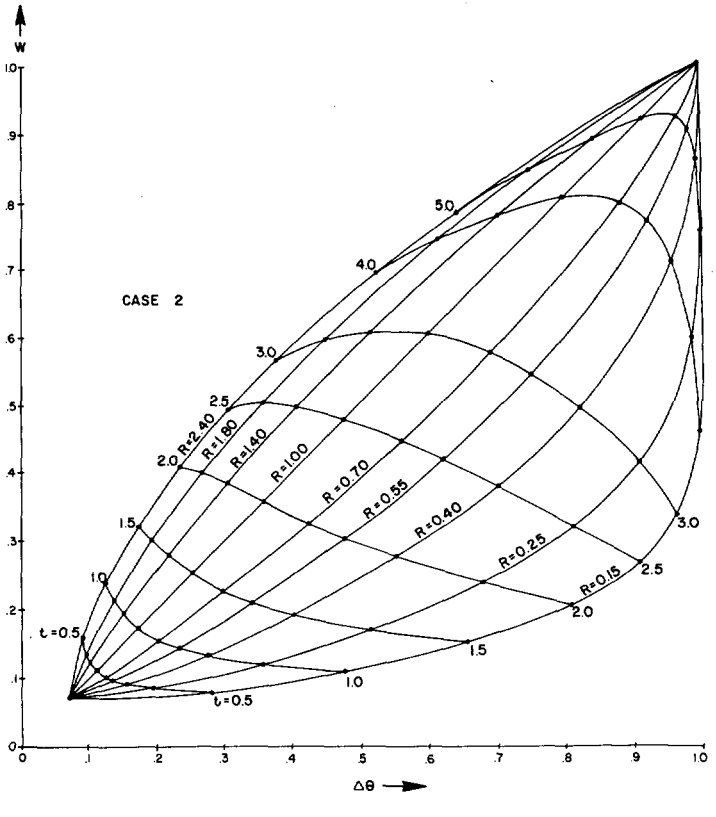

FIGURE 5.—Convection solutions for case 2.

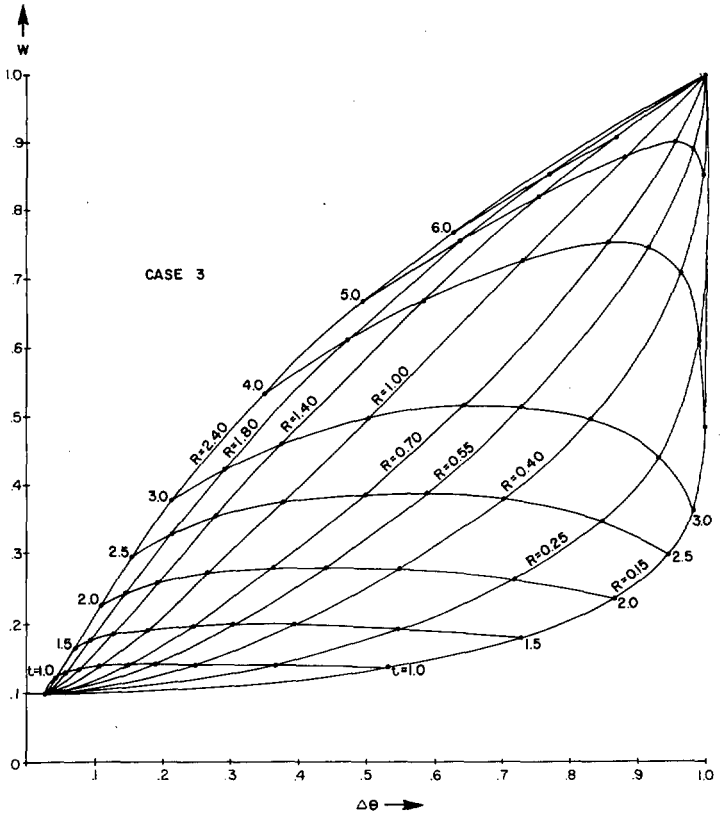

FIGURE 6.—Convection solutions for case 3.

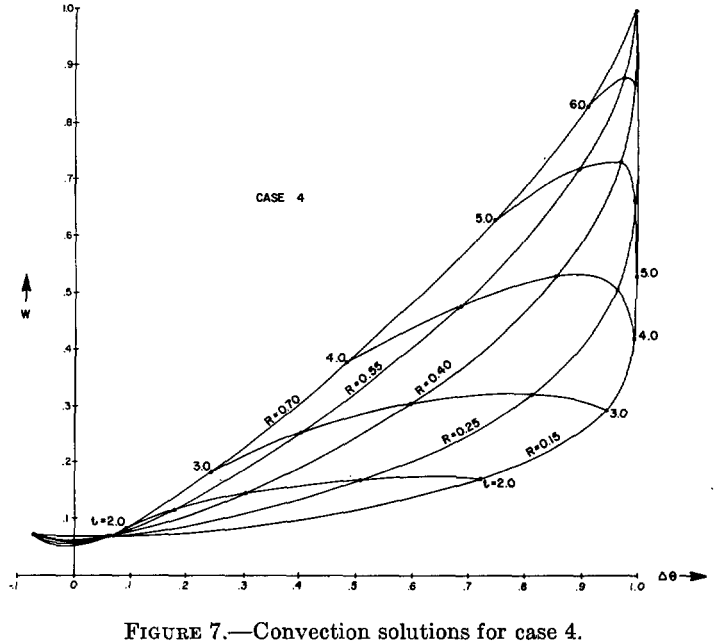

FIGURE 7.—Convection solutions for case 4.

together with inertia cause the deceleration to persist. The plumelike updrafts have generated most of the temperature excess when this phenomenon appears, and the undershoot does not exceed about 10 percent. When $R=2.40$, the undershoot already appears before the

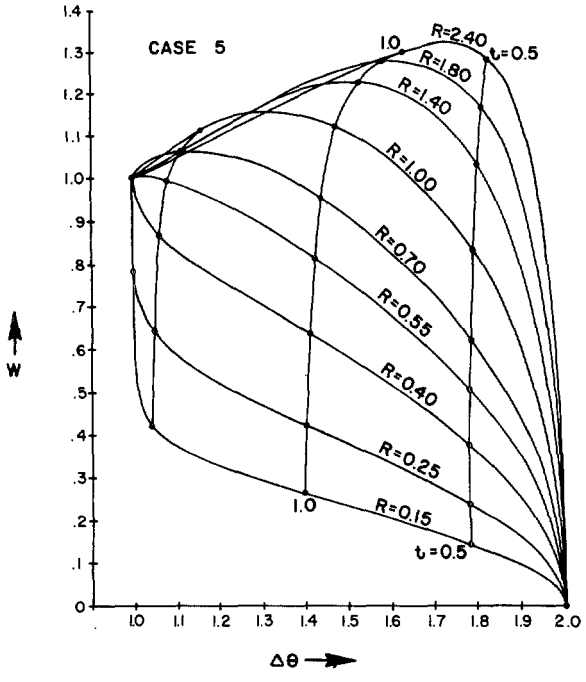

FIGURE 8.—Convection solutions for case 5.

temperature difference has attained 15 percent of the steady-state value, and reaches close to 50 percent.

Finally, in case 8 as in case 4, steady-state convection develops in the initially cold updraft only if $R<1$. For the two smallest values of R, associated with large steady-state velocities, the rapid release of latent heat brought about by the even faster initial updraft reverses the radial temperature field soon enough so that W remains greater than 1 at all times. Beyond a critical value of R close to 0.40, an undershoot in W appears as the temperature field reverses too slowly to counteract the inhibiting negative buoyancy. As R approaches unity, the undershoot becomes more pronounced and appears earlier. When $R=0.70$, the phenomenon occurs while the updraft is still colder than the downdraft. As in case 4, the plume-like updrafts are almost completely damped out by the unfavorable temperature field before reversing toward the steady state; when $R=1$, $\Delta\theta=-W$ at all times. The initial negative buoyancy can no longer be overcome by the updraft, which decays toward the rest state. For the same reason stated in case 4, the solutions of equations (16) and (17) have no physical meaning if R is larger than 1.

6. SUMMARY AND CONCLUSIONS

In Asai's model of cellular cumulus convection, the early growth rate of small initial perturbations from rest increases with the degree of conditional instability and shows approximately direct variation with the steady-state upward heat transport if the horizontal scale of the updraft is comparable to or larger than its vertical scale. Plume-like updrafts within cells of small horizontal scale have the most rapid growth.

For either small or large initial perturbations (relative to steady-state values), it appears that steady-state convection develops under any of the following initial conditions:

1) temperature excess with no vertical motion,
2) both upward motion and temperature excess, and
3) upward motion with no temperature excess.

Beyond the early growth states, the mode of approach toward steady state for small initial perturbations is nearly independent of the initial conditions for a given combination of cell geometry, entrainment rate, and conditional instability. In broad updrafts with low steady-state vertical velocities, the development of temperature excess lags behind the updraft development, while the opposite holds for narrow updrafts with high steady state velocities. When the horizontal and vertical scales of the updraft are markedly different, large initial heating without vertical motion creates sufficient buoyancy to accelerate the updraft temporarily beyond the steady-state speed. On the other hand, with no initial heating but upward motion faster than the steady-state, currents with low absolute velocities temporarily undershoot the equilibrium velocity due to the small thermal buoyancy.

Initial upward motion with a negative temperature perturbation supports the development of steady-state convection provided the entrainment rate and updraft width (relative to the total cell width) are sufficiently small. Horizontal mixing is then small, so that the latent heat release resulting from the initial upward push can overcome the negative buoyancy. If these conditions are not satisfied, there is either no physically meaningful convection, or singular damping to the rest state occurs.

ACKNOWLEDGMENTS

This research was supported under ESSA Grant E-230-68-G to the Space Science and Engineering Center at the University of Wisconsin. Computer time was provided by W.A.R.F. funds through the University Research Committee. Figures were prepared by Mr. Tony Wendricks.

REFERENCES

Asai, Tomio, "On the Characteristics of Cellular Cumulus Convection," *Journal of the Meteorological Society of Japan*, Ser. 2, Vol. 45, No. 3, June **1967**, pp. 251–260.

Kuo, H. L., "On the Controlling Influences of Eddy Diffusion on Thermal Convection," *Journal of the Atmospheric Sciences*, Vol. 19, No. 3, May **1962**, pp. 236–243.

Ogura, Yoshimitsu, "The Evolution of a Moist Convective Element in a Shallow, Conditionally Unstable Atmosphere: A Numerical Calculation," *Journal of the Atmospheric Sciences*, Vol. 20, No. 5, Sept. **1963**, pp. 407–424.

Saltzman, Barry, "Finite Amplitude Free Convection as an Initial Value Problem—I," *Journal of the Atmospheric Sciences*, Vol. 19, No. 4, July **1962**, pp. 329–341.

[*Received September 2, 1969; revised November 24, 1969*]